Uncertainty Quantification in Modeling and Measuring Components with Resonant Ultrasound Spectroscopy

Eric Biedermann[2, a)], Leanne Jauriqui[2, b)], John C. Aldrin[3,c)], Alexander Mayes[2,d)], Tom Williams[2,e)], Siamack Mazdiyasni[1,f)]

[1]*Air Force Research Laboratory (AFRL/RXCA), Wright-Patterson AFB, OH 45433, USA*
[2]*Vibrant Corporation, Albuquerque, NM 87113, USA*
[3]*Computational Tools, Gurnee, IL 60031, USA*

[a)] *Eric Biedermann: ebiedermann@vibrantndt.com*
[b)] *Leanne Jauriqui: ljauriqui@vibrantndt.com*
[c)] *John Aldrin: aldrin@computationaltools.com*
[d)] *Alexander Mayes: amayes@vibrantndt.com*
[e)] *Tom Williams: twilliams@vibrantndt.com*
[f)] *Siamack Mazdiyasni: siamack.mazdiyasni@us.af.mil*

Abstract. Resonant Ultrasound Spectroscopy (RUS) is a nondestructive evaluation (NDE) method which can be used for material characterization, defect detection, process control and life monitoring for critical components in gas turbine engines, aircraft and other systems. Accurate forward and inverse modeling for RUS requires a proper accounting of the propagation of uncertainty due to the model and measurement sources. A process for quantifying the propagation of uncertainty to RUS frequency results for models and measurements was developed. Epistemic and aleatory sources of uncertainty were identified for forward model parameters, forward model material property and geometry inputs, inverse model parameters, and physical RUS measurements. RUS model parametric studies were then conducted for simple geometric samples to determine the sensitivity of RUS frequencies and model inversion results to the various sources of uncertainty. The results of these parametric studies were used to calculate uncertainty bounds associated with each source. Uncertainty bounds were then compared to assess the relative impact of the various sources of uncertainty, and mitigations were identified. The elastic material property inputs for forward models, such as Young's Modulus, were found to be the most significant source of uncertainty in these studies. The end result of this work was the development of an uncertainty quantification process that can be adapted to a broad range of components and materials.

INTRODUCTION

Resonant Ultrasound Spectroscopy (RUS) is a method for non-destructive evaluation (NDE) and material characterization that uses the ultrasonic resonance frequencies of a component [1]. Vibrant Corporation combines RUS with advanced pattern recognition algorithms and statistical scoring to field Process Compensated Resonance Testing (PCRT) for commercial NDE applications [2]. Among the most critical of those applications are gas turbine engine blades made from nickel-based superalloys [3]. FIGURE 1(a) shows a turbine blade from the JT8D turbofan engine on a PCRT test fixture. In testing of turbine blades, Vibrant has demonstrated sensitivity of resonance frequencies to material conditions, such as over-temperature exposure, that reduce creep resistance in the Ni-base superalloy material. FIGURE 1(b) shows the sensitivity of resonance frequencies to increasing exposure temperatures. PCRT NDE applications for blade over-temperature have earned FAA approval [4], replacing destructive cut-up sampling of one blade from a suspect engine set with a nondestructive test that inspects each blade individually.

(a)

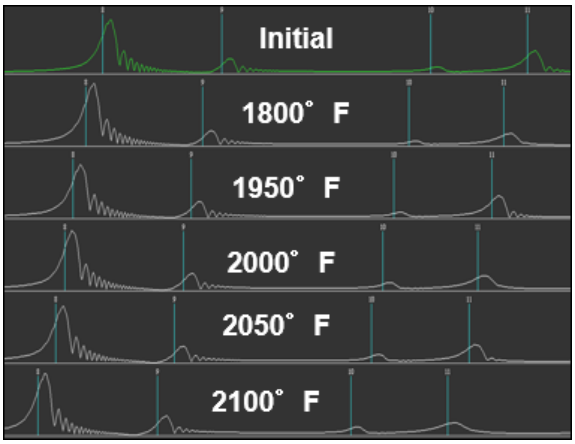

(b)

FIGURE 1. Vibrant experience with RUS for Ni-base superalloy, (a) JT8D turbine blade on PCRT test fixture, (b) frequency sensitivity to over-temperature exposure

Historically, RUS-based inspections require the collection of a large quantity of empirical data in the form of resonance frequencies and part classifications to serve as a training set. Going forward, there is a critical need for quantitative models to more precisely relate changes in the material state, ideally from the micro and the macro-scales, with the resonance behavior of the material. As turbine engines age and lose exhaust gas temperature margin, the combined temperature and stress on the airfoils eventually cause the airfoil microstructure to undergo gradual changes resulting in a reduction of strength and creep resistance. Prior work on gas turbine airfoils exposed to high temperature and stress has shown that RUS is capable of measuring consistent correlated shifts in resonance frequency peaks [3-4]. However, it should be recognized that in real engineered structures, such as gas turbine engines, multiple damage mechanisms often occur simultaneously, confounding the interpretation of the shift in frequency peaks.

A team led by Vibrant and the Air Force Research Laboratory is developing tools and techniques for RUS forward modeling and model inversion [5-6]. The goal is to more precisely connect changes in the resonance frequencies of nickel-based superalloy components to the component material and damage state. Accurate forward and inverse modeling of RUS requires a proper accounting of propagation of uncertainty due to model, material and measurement errors. Once sources of error are identified, the uncertainty propagation due to those errors must be quantified and addressed as needed.

RUS MODELING

Recent work on RUS modeling [5-6] has led to significant developments in forward and inverse RUS models. FIGURE 2 shows a diagram on forward modeling and model-based inversion in the RUS context. A forward model takes what is known about a part to predict its resonance frequencies and mode shapes. The components of the forward model include part geometry, macro-scale material properties, material microstructure, material state model, internal stress state and RUS test conditions. Model inversion connects measured changes in the resonance frequencies of parts under test to a quantitative evaluation of the macro-scale test specimen, micro-structure material state and ideally, life prediction. RUS property inversion tools have also been developed in Matlab to provide quantitative inversion capability. The conventional RUS inversion algorithms have been enhanced with the addition of parameters to simulate asymmetry in material properties and changes in geometry due to creep and other loads. An inversion capability using surrogate models from finite element method (FEM) data has also been developed. FEM model-based inversion provides greater flexibility for evaluating crystal orientation, complex geometries and localized defects.

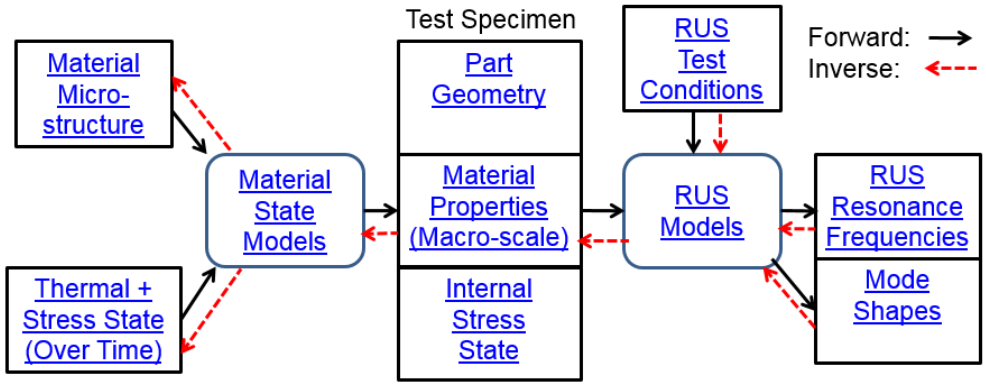

FIGURE 2. RUS forward modeling and model inversion

UNCERTAINTY ANALYSIS

The quantification analyses performed in this project were concerned with two forms of uncertainty, aleatory and epistemic. Aleatory uncertainty characterizes the inherent randomness in the behavior of a system under study. It can be quantified with sensitivity analyses. Examples of aleatory uncertainty for RUS modeling include variation in material properties, material processing parameters, geometric dimensions and shot-to-shot variation in RUS frequency measurements.

Epistemic uncertainty characterizes a lack of knowledge about the appropriate value to use for a quantity assumed to have a fixed value. Examples of epistemic uncertainty for RUS modeling include mesh parameters in FEM solutions and model inversion parameters such as polynomial order, mode range and output constraints.

Quantifying uncertainty in the model and measurement results required identification of sources of error that contribute to uncertainty. Four categories of error were identified:

1. Forward modeling technique: Describes parameters for running forward models, such as analytical model polynomial order and FEM model mesh resolution. This was considered a type of epistemic uncertainty, with optimal values for these parameters that could be found and used as a best practice.
2. Forward model inputs: Describes variation in inputs for forward models, such as material model (iso, cubic, etc.) material properties and geometric dimensions. Other inputs could be global or local material stress state and defect characteristics. These were considered sources of aleatory uncertainty / random variation. To manage the project scope, the project focused on material property variation within published limits for baseline Mar-M-247, and geometric dimensions within the machining tolerances for the samples.
3. Inverse modeling: Describes variation in inputs for inverse models. Many of these were considered epistemic with optimal values for a given geometry and material type. However, model inversion also includes aleatory uncertainty. Inversion requires an input set of measured resonance frequencies, and the variation in those frequencies will have an effect on the inversion results.
4. RUS measurements: Describes variation in measured resonance frequencies. RUS measurements have a mix of epistemic and aleatory uncertainty. Epistemic sources included fixturing (two-point, three-point or four-point, for example). Aleatory sources included shot-to-shot, part-to-part, and transducer variation.

FORWARD MODEL UNCERTAINTY

A series of forward model One-Factor-At-a-Time (OFAT) parametric studies were performed using a finite element model of a cylindrical coupon. These studies varied geometric (length and diameter) dimensions and Mar-M-247 material properties (elastic properties and density) and recorded the sensitivity of resonance frequencies to those variations. Simulations were run for isotropic and cubic material models. Two sets of baseline values were used for each material type, for a total of four parametric studies. The isotropic material models used Young's Modulus (E) and Poisson's ratio (ν) for material inputs. The cubic model used elastic constants C11, C12, and C44 from the elastic constant matrix that relates stress and strain tensors according to the theory of elasticity [7].

Each material model used two baseline sets of material properties and two ranges for variation in the material properties. The first set came from Kuhn & Sockel [8], while the other was an average result of RUS inversion models. The baseline values in both material models were relatively similar, but the ranges of variation for E and ν defined by each model were significantly different. The Kuhn & Sockel model set the range of variation in both E and ν at +/- 5%. The average results from the inversion model for a set of 42 specimens had a smaller range of E variation (+/- 2%) but significantly larger ν variation (+/-10% for isotropic and +/-7% for cubic). Geometric variation was assumed to be within the tolerances established by the drawings for the cylindrical samples. The cubic model included the anisotropy ratio A. TABLE 1 shows the material and geometry input ranges for this study.

TABLE 1. Material/geometry input parameter ranges for forward model cases; *Cubic E, ν, and A derived from Cxy values

	Iso – Kuhn & Sockel	**Iso – Inversion Average**	**Cubic – Kuhn & Sockel**	**Cubic – Inversion Average**
E	219.3 GPa, +/-5%	212.0 GPa, +/-2%	126.8 GPa*, +/-5%	127.8 GPa*, +/-2%
ν	0.32, +/-5%	0.31, +/-10%	0.39*, +/-5%	0.37*, +/-7%
ρ	8.55 g/cm^3, +/-0.2%	8.55 g/cm^3, +/-0.2%	8.55 g/cm^3, +/-0.2%	8.55 g/cm^3, +/-0.2%
L	3.0 in., +/- 0.066%	3.0 in., +/- 0.066%	3.0 in., +/- 0.066%	3.0 in., +/- 0.066%
D	0.5 in., +/-0.039%	0.5in., +/-0.039%	0.5 in., +/-0.039%	0.5 in., +/-0.039%
A	N/A	N/A	2.75*, +/-5%	2.75*, +/-5%

The resonance frequency changes and mode shapes were tracked to ensure that mode swapping did not confound the analysis. FIGURE 3 shows the frequency changes for the isotropic Kuhn & Sockel baseline model. Changes to E and density produce uniform changes to resonance frequencies, but geometric and ν variation causes pattern shifts that indicates variation in mode shape sensitivity to these parameters. For example, torsional modes show the greatest sensitivity to changes in ν. This is in line with previous experience with forward model parametric studies.

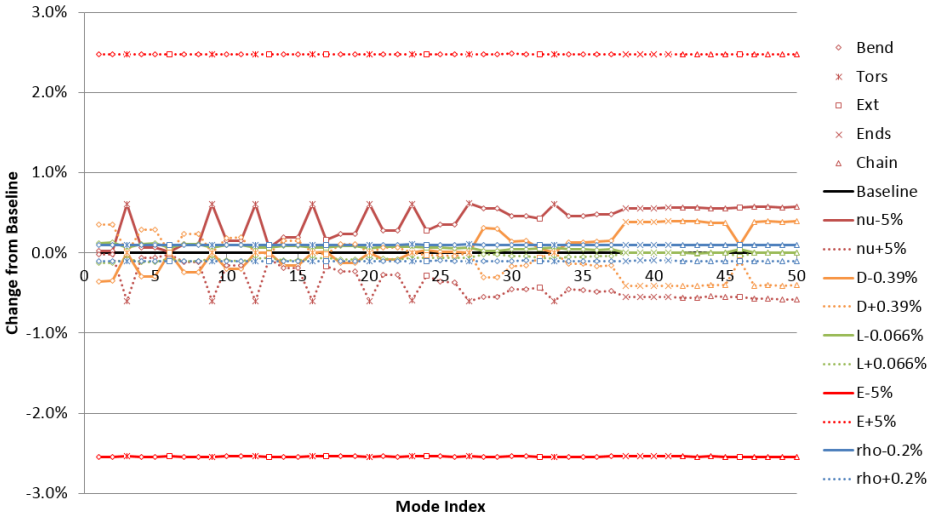

FIGURE 3. Frequency changes vs. variation in material and geometric parameters with mode shape types identified, Kuhn & Sockel isotropic baseline properties

The results of sensitivity studies were used to calculate uncertainty bounds for the distributions for resonance results from models. These bounds assumed 3σ normal distributions for the material and geometric properties. For all uncertainty plots, the thin black line represents the full range of variation for a given parameter. The blue bar represents the interquartile range between the first and third quartiles, centered on the median value. The uncertainty bounds were calculated for each input parameter for representative mode shapes (low-order bend, torsion, extensional and

high-order bend). Overall, the bounds were wider for the mode shapes that were more sensitive to the model parameter in question, such as torsional modes vs. ν. The uniformly high sensitivity to variation in E, and the relatively large range of E variation from Kuhn & Sockel led to significant uncertainty propagation relative to other parameters.

For the low-order bending modes, the cylinder diameter was a distant second for propagation of uncertainty in the resonance frequencies (FIGURE 4(a)). Torsional modes show higher sensitivity to ν, leading to wider ν bounds for that mode class vs. others mode shapes (FIGURE 4(b)). The torsional mode is insensitive to variation in diameter.

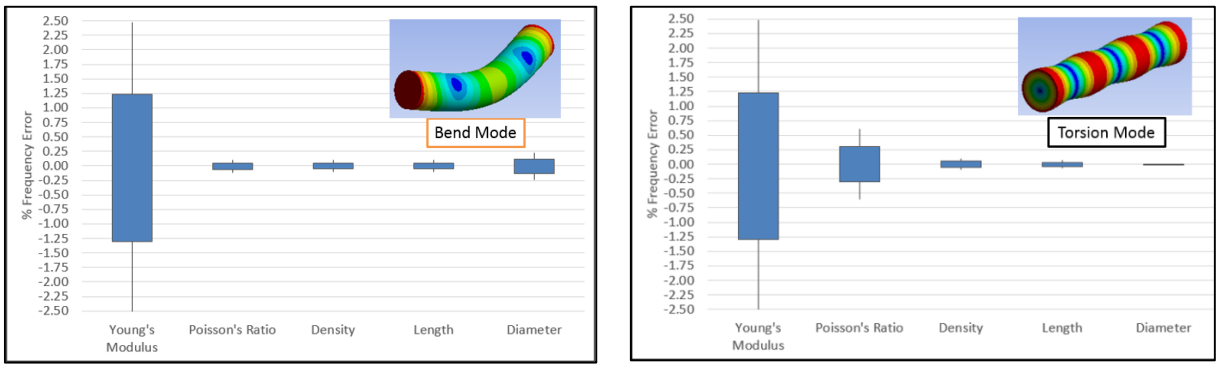

(a) (b)

FIGURE 4. Frequency uncertainty bounds vs. material input parameter for cylinder with Kuhn & Sockel baseline isotropic material model, (a) low-order bending mode, (b) low-order torsional mode

After the OFAT sensitivity and uncertainty propagation were established, scenarios with coupled parameter variation were examined. A Monte Carlo analysis calculated uncertainty bounds for forward models with simultaneous variation in modulus, density, Poisson's ratio, length and diameter. The isotropic material model with Kuhn & Sockel baseline parameters was used for this study. Each parameter was assumed to have a 3σ normal distribution within the bounds established by the "Iso – Kuhn & Sockel" column in TABLE 1. The material and geometry input values were pulled randomly from the normal distributions for each case. The Monte Carlo analysis used 100 design points.

FIGURE 5 shows the results of the Monte Carlo analysis with all material and geometric parameters coupled (a) and with modulus excluded (b). The black line represents the median frequency change versus baseline. The blue band is the 0.25 to 0.75 percentile of the full range of variation. The green band is the 0.10 to 0.90 percentile of the full range. The pattern of the median and bands reflected a combination of the bulk change associated with variation in modulus and density and the pattern changes from Poisson's ratio and geometric variation. The Monte Carlo data indicated that overall uncertainty due to modulus far outweighed the effect of other parameters as in the OFAT results. Reducing uncertainty in modulus would yield the biggest in uncertainty for these modeled scenarios.

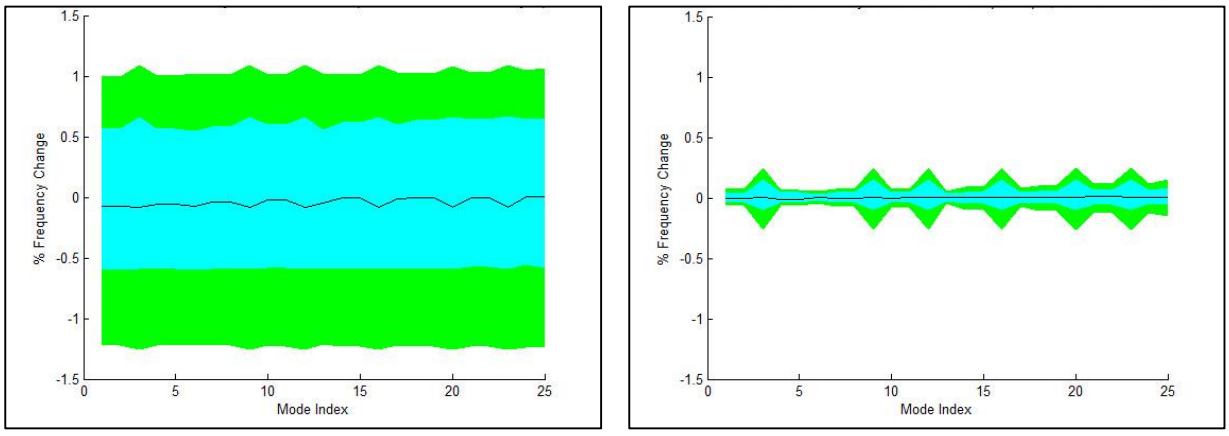

(a) (b)

FIGURE 5. (a) Monte Carlo simulation results for all parameters coupled. (b) Monte Carlo simulation results with modulus excluded. Black line: median frequency change vs. baseline; blue band: 0.25 to 0.75 percentile of full range of variation; green band: 0.10 to 0.90 percentile of full range of variation

MODEL INVERSION UNCERTAINTY

Model inversion requires a set of 'target' resonance frequencies, either from a measurement or alternate model. Inverting for elastic properties requires the number of parameters to fit (two for isotropic, three for cubic, etc.) and an estimate of the material properties of the sample, specified in C_{xy} format. The best-fit approach, i.e. fit to C_{xy} or engineering values (E, ν, A) and Polynomial Order (PO) for the fit must be specified. Ranges or values for output constraints and number of validation iterations may also be required.

Sets of FEM output frequencies for known input conditions were used as input to the inverse analytical model engines. The inversion model was evaluated in both isotropic and cubic modes for both the C_{xy} and engineering property (E, ν, A) approaches. The FEM modeled frequencies and analytical model frequencies were very well aligned. FIGURE 6 shows a comparison of polynomial order analytical modes to an FEM model. Modeled frequencies are a good match for all polynomial orders through the first 16 modes. The 16th order analytical model was well-matched through 30 modes, the 18th order through 42 modes, and the 20th order was well-matched through 60 modes.

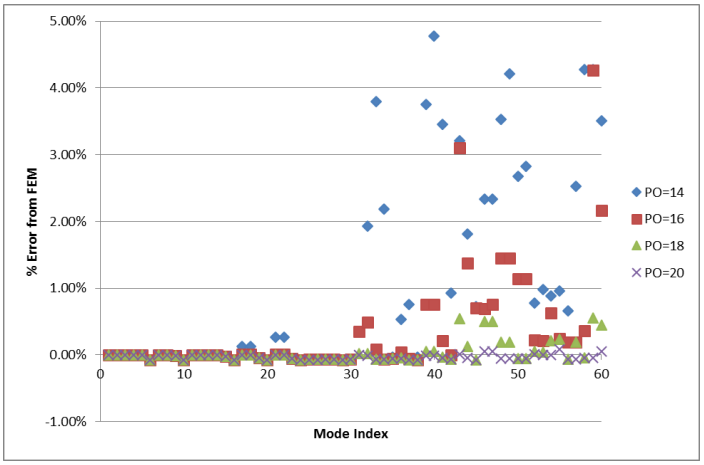

FIGURE 6. Error between FEM and analytical models for various polynomial order analytical models.

The selection of resonant modes evaluated in the inversion is another critical parameter. Uncertainty propagation on inversion results from using different peak sets was evaluated. The FEM modeled frequencies were inverted 5 times with each peak set to verify convergence. FIGURE 7 shows the best-fit error relative to the C11 value for the 'target' FEM model. Nearly all results converged to within 5% of the actual values. Inversion of peaks 1-40 led to inconsistent results, despite the match of these modeled frequencies to the FEM input for polynomial orders greater than 16. The results for polynomial order 18 were the most accurate, with the narrowest confidence bounds. Peak sets 1-20 and 1-30 produce very similar results, but 1-20 had an overall better fit to the FEM target data.

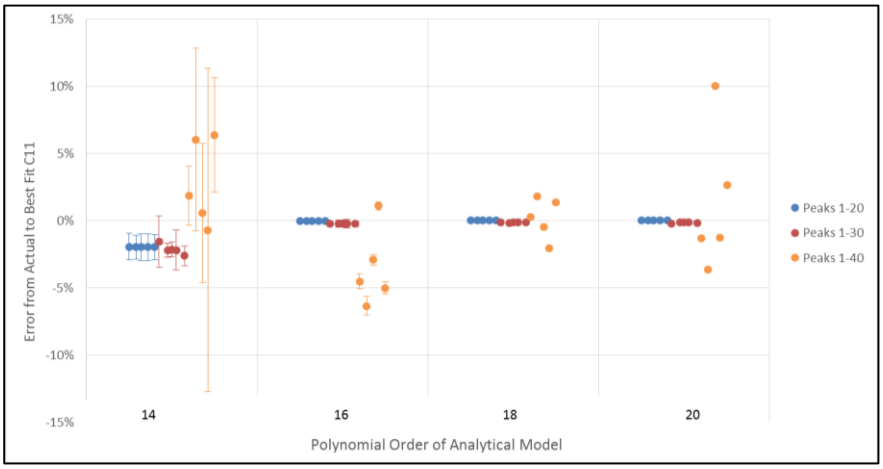

FIGURE 7. Best-fit C11 values for inversion models of cubic material using various peak sets. (C11 target value 246 GPa)

Uncertainty bounds were calculated for model inversion using various peak sets for PO = 16 (FIGURE 8). The uncertainty values were calculated from 30 repeat inversions of the FEM-generated frequency set. The uncertainty bounds for the Peaks 1-40 scenario were significantly greater than for Peaks 1-30 and Peaks 1-20.

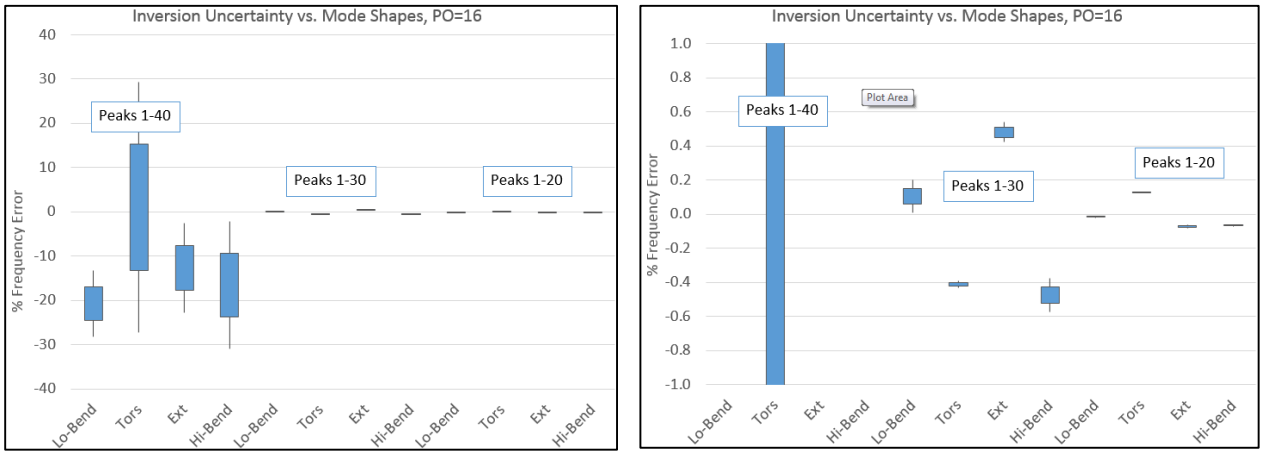

(a) (b)

FIGURE 8. **(a)** Frequency error from inversion for different peak sets, PO=16, (b) Detail view of Peaks 1-20 and 1-30

RUS MEASUREMENT UNCERTAINTY STUDIES

A study was conducted of the RUS/PCRT measurement variation using resonance measurements for ½" diameter by 3" long cylindrical Mar-M247 coupons. Resonance data were collected for 42 modes between 20 and 180 kHz, under a variety of conditions. Among the conditions examined were RUS fixturing variables, such as two-point vs. four-point configurations (FIGURE 9) and multiple transducer sets.

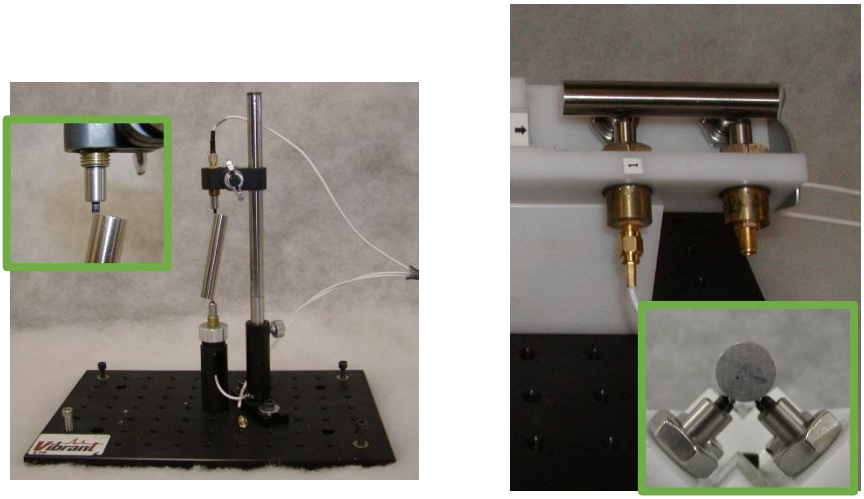

FIGURE 9. PCRT fixtures used for repeat measurement studies of cylindrical coupons; two-point fixture (left), and four-point v-block (right)

FIGURE 10(a) shows the repeatability of the data for a 'four-point' v-block fixture, as shown in FIGURE 9. Thirty measurements were taken statically, with the sample remaining on the fixture. Thirty measurements were then taken with re-mounting between each measurement. While the standard deviation of measurements for the re-mount mode was nearly five times greater (0.023% compared to 0.0048%), and the '90% range' was three times greater, accommodating the error associated with re-mount was necessary for the comparison of multiple coupons. In the re-mount mode, 96.6% of repeat measurements were still within +/- 0.03% of the average. Comparison of two-point and

four-point fixtures with re-mount found that the two-point fixture had 1.5 times the variability of the four-point, but the absolute deviation for both was still very low (FIGURE 10(b)).

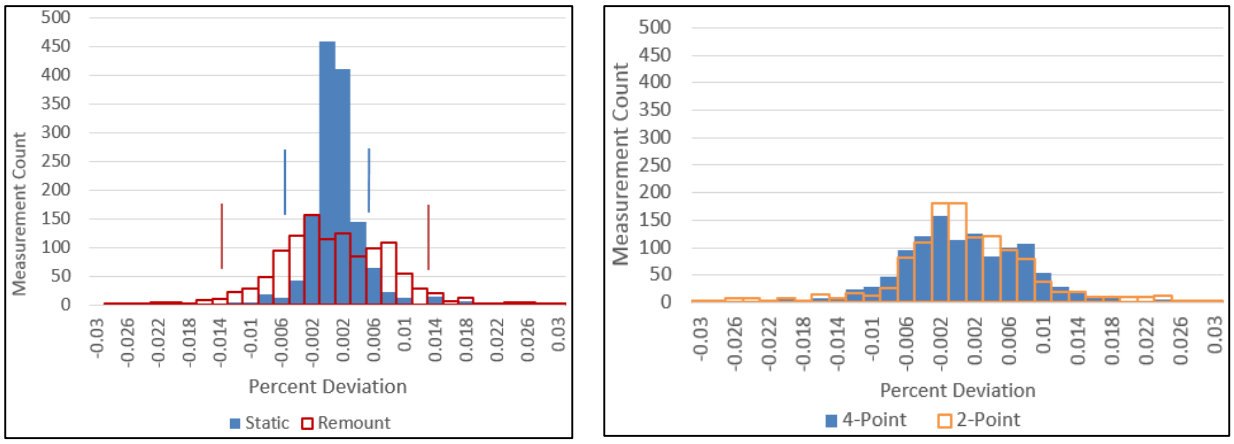

(a) (b)

FIGURE 10. (a) Shot-to-shot resonance frequency measurement deviations in four-point fixture, (b) comparison of shot-to-shot resonance frequency deviations for different fixtures

The repeatability for a single sample was compared to the sample-sample variability. Forty-two samples of EQ Mar-M-247 were available for this comparison. FIGURE 11 shows averaged frequency data (more than 40 modes of vibration) for shot-to-shot variation of a single sample for two different transducer sets in the four-point fixture overlaid onto data for the 42-sample population. While the cumulative effect of all resonances evaluated led to a standard deviation of the full coupon population eleven times greater than the deviation of measurements for a single sample, some individual resonances showed differences of 50X or greater. PCRT Gage R&R studies routinely show that part-part variation makes shot-to-shot variation nearly negligible, with %R&R values of less than 2% [6].

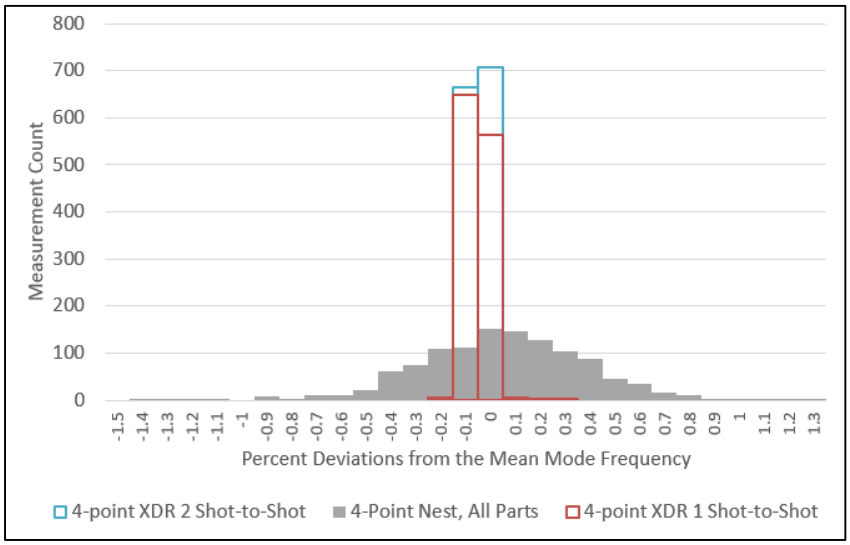

FIGURE 11. Percent deviation from 42-peak mode mean frequency, shot-to-shot deviations vs. sample-sample

UNCERTAINTY BOUND COMPARISONS

Comparisons of the various sources of uncertainty (forward model, inversion model, measurement) were made to identify the most significant contributors. The goal was to highlight where the most improvement in model accuracy could be made. FIGURE 12 shows a comparison between uncertainty in inversion models, forward models due to elastic modulus (*E*) variation, forward models due to diameter error, and RUS/PCRT measurement error for various

mode shapes. These represent the worst cases, or highest error sources. In this comparison the Peaks 1-40 inversion case was excluded because it was simply too variable to be considered viable, so the Peaks 1-30 case was used instead. The forward model uncertainty bounds from *E* variation dwarfed those of the other forward model inputs, inversion models, and physical measurements. This high sensitivity to Young's modulus and even other part characteristics like diameter and Poisson's ratio indicate RUS has the capability to resolve these characteristics with respect to PCRT measurement error.

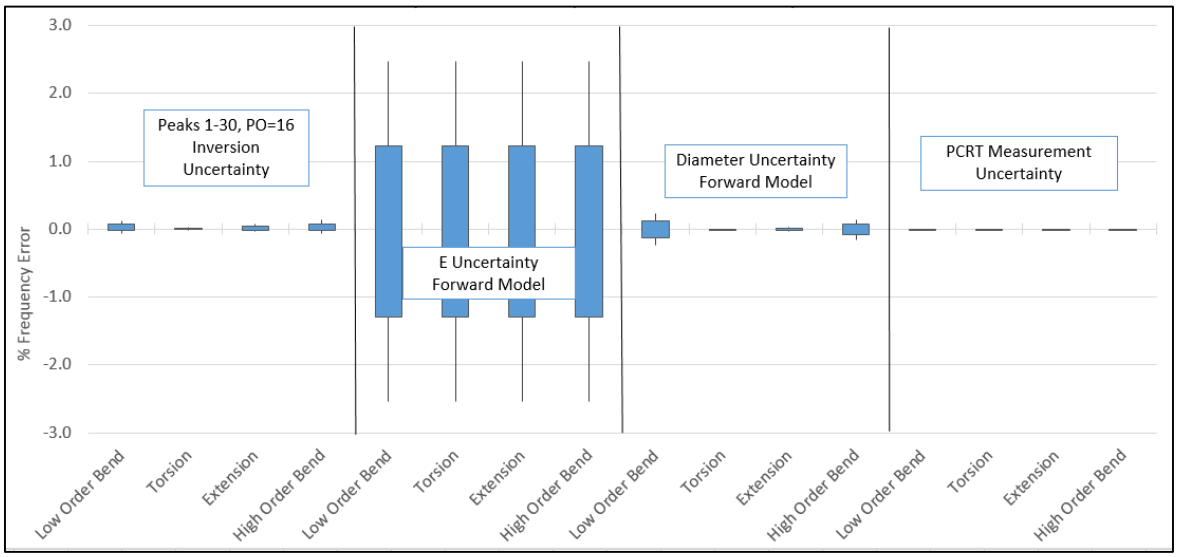

FIGURE 12. Resonance frequency uncertainty comparison, from left to right: Inversion using peaks 1-30, forward model due to E, forward model due to diameter, measurement

FIGURE 13 compares uncertainty bounds for lower error scenarios, including inversion model uncertainty (this time for Peaks 1-20), forward models due to Poisson's ratio (ν) uncertainty, forward models due to length uncertainty and RUS/PCRT measurement uncertainty. The forward model uncertainty bounds from ν uncertainty were easily the widest. However the largest uncertainty bounds for ν (-0.60% to +0.60%) were still only a fraction of those for *E* (uniformly +/-2.5%) from FIGURE 12.

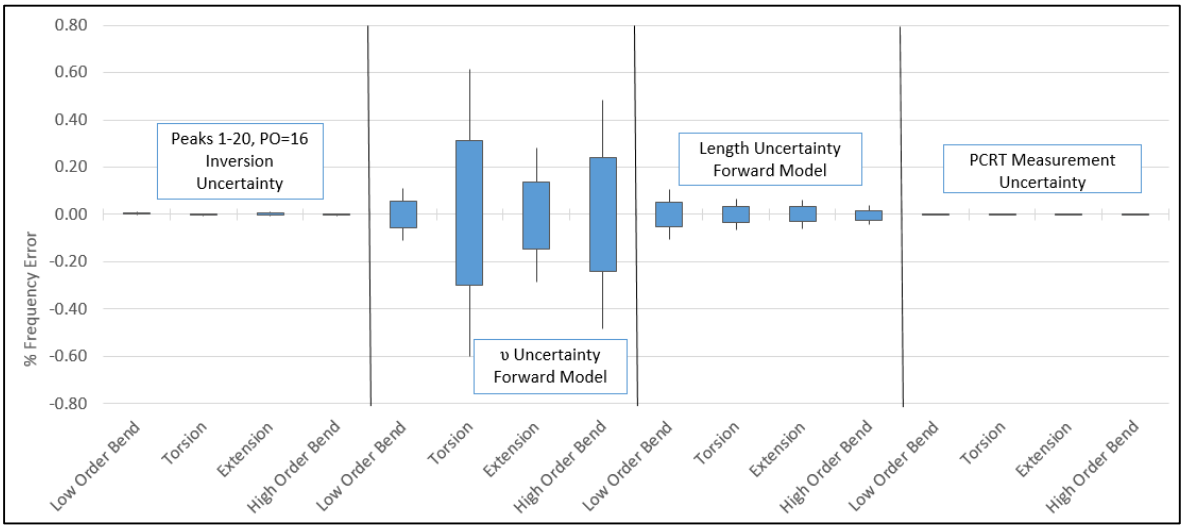

FIGURE 13. Uncertainty comparison, from left to right: Inversion using peaks 1-20, forward model due to ν, forward model due to length, measurement

The uncertainty bound comparisons illustrated that uncertainty in forward model output due to uncertainty in the input material parameters as defined in [8] was the single largest source of error. Reducing the range of variation for the forward model material inputs would lead to a significant reduction in forward model output uncertainty.

Uncertainty in the geometric dimensions of the samples was a distant second to material uncertainty. The relatively tight tolerances of the machining drawings that defined the cylinder samples helped to reduce geometry's effect on overall output uncertainty. Dimensions for relevant features with wider tolerances, such as as-cast surfaces on turbine blades, would be expected to produce wider uncertainty bounds.

The error contributed by the RUS/PCRT measurements is nearly negligible, and the error associated with the inversion is small, for the well-posed inversion problem. Some of the scenarios evaluated would lead to much larger error, so inversion metrics should definitely be observed in evaluating results.

CONCLUSIONS AND FUTURE WORK

A UQ process was developed and demonstrated that effectively calculates and compares uncertainty bounds for various sources of error. Comparison of uncertainty from each source identifies the most significant sources, and enables identification of mitigation. The basic steps in this process can be summarized as follows: (1) identify sources of uncertainty, (2) study forward model parameter sensitivity and identify epistemic values for optimal accuracy, (3) study forward model sensitivity to material, geometric and other inputs, and quantify uncertainty, (4) quantify inversion uncertainty, (5) quantify measurement uncertainty, and (6) compare uncertainty from each source and identify any necessary steps for mitigation. For this demonstration, the material input parameters for forward models, especially E and ν, were found to be the largest sources of uncertainty among the sources studied in RUS models and measurements. Addressing this variability through more effective material characterization, including well-posed RUS model inversion, may be an effective mitigation. Future work will expand the application of the UQ process to a wider array of component geometries and material states, and ideally include representative turbine hardware and relevant damage mechanisms.

ACKNOWLEDGMENTS

This work was supported by the U.S. Air Force Research Laboratory (AFRL) through a Small Business Innovation Research (SBIR) Phase I Contract, FA8650-14-M-5034. This paper has been cleared for public release by AFRL under case number 88ABW-2015-4932.

REFERENCES

1. Migliori, A., Sarrao, J., Visscher, M. W., Bell, T., Lei, M., Fisk, Z., and Leisure, R., ''Resonant ultrasound spectroscopy techniques for measurement of the elastic moduli of solids,'' *Physica B*, **183**, 1–24 (1993).
2. Schwarz, J., Saxton, J., and Jauriqui, L., "Process Compensated Resonant Testing in Manufacturing Process Control," *Material Evaluation*, **63** 736-739, (July 2005).
3. Piotrowski, D., Hunter, L., and Sloan, T., "Process Compensated Resonance Testing JT8D-219 1st Stage Blades," ATA NDT Forum 2008, (September 24, 2008). [http://www.vibrantndt.co.uk/files/2008_ATA_NDT_Forum-PCRT_of_JT8D-T1_Blades.pdf].
4. Federal Aviation Administration, Atlanta Aircraft Certification Office (2010). A/W File No.: G2010-07 5087.
5. Biedermann, E., Jauriqui, L., Aldrin, J. C., Goodlet, B., Pollock, T., Torbet, C., Mazdiyasni, S., "Resonance Ultrasound Spectroscopy Forward Modeling and Inverse Characterization of Nickel-Based Superalloys," *Review of Progress in QNDE,* Vol. 34, AIP, pp. 835-844, (2015).
6. Biedermann, E., Jauriqui, L., Aldrin, J. C., Goodlet, B., Pollock, T., Torbet, C., "Understanding of Resonance Ultrasound Spectroscopy Signature in Precipitate Coarsening of Nickel-Base Superalloy," AFRL-RX-WP-TR-20140-0237, (2014).
7. Gould, P. L., *Introduction to Linear Elasticity*. New York: Springer, (1994).
8. Kuhn, H-A. and Sockel, H-G, "Elastic Properties of Textured and Directionally Solidified Nickel-based Superalloys Between 25 and 1200° C," *Materials Science and Engineering, A112,* 177-126, (1989).